Proc. Natl. Acad. Sci. USA
Vol. 95, pp. 15223–15228, December 1998
Biochemistry

Interaction of the Hsp70 molecular chaperone, DnaK, with its cochaperone DnaJ

WON-CHUL SUH*, WILLIAM F. BURKHOLDER†‡, CHI ZEN LU*, XUN ZHAO†, MAX E. GOTTESMAN†, AND CAROL A. GROSS*§

*Departments of Microbiology and Stomatology, University of California, San Francisco, CA 94143; and †Department of Biochemistry and Molecular Biophysics, College of Physicians and Surgeons, Columbia University, New York, NY 10032

Contributed by Carol A. Gross, October 20, 1998

ABSTRACT **Chaperones of the Hsp70 family bind to unfolded or partially folded polypeptides to facilitate many cellular processes. ATP hydrolysis and substrate binding, the two key molecular activities of this chaperone, are modulated by the cochaperone DnaJ. By using both genetic and biochemical approaches, we provide evidence that DnaJ binds to at least two sites on the *Escherichia coli* Hsp70 family member DnaK: under the ATPase domain in a cleft between its two subdomains and at or near the pocket of substrate binding. The lower cleft of the ATPase domain is defined as a binding pocket for the J-domain because (*i*) a DnaK mutation located in this cleft (R167H) is an allele-specific suppressor of the binding defect of the DnaJ mutation, D35N and (*ii*) alanine substitution of two residues close to R167 in the crystal structure, N170A and T173A, significantly decrease DnaJ binding. A second binding determinant is likely to be in the substrate-binding domain because some DnaK mutations in the vicinity of the substrate-binding pocket are defective in either the affinity (G400D, G539D) or rate (D526N) of both peptide and DnaJ binding to DnaK. Binding of DnaJ may propagate conformational changes to the nearby ATPase catalytic center and substrate-binding sites as well as facilitate communication between these two domains to alter the molecular properties of Hsp70.**

Molecular chaperones of the Hsp70 family are conserved proteins that modulate intracellular protein folding. By binding to unfolded or partially folded polypeptides, chaperones prevent misfolding and aggregation and promote folding, translocation, and the assembly and disassembly of multiprotein structures (1, 2). Both prokaryotes and eukaryotes have multiple Hsp70 proteins that function in diverse processes. Hsp70s have a highly conserved 44-kDa ATPase domain followed by a highly conserved 15-kDa peptide-binding domain and a less conserved 10-kDa C-terminal region. The structures of the two conserved domains have been determined separately by x-ray crystallography (3, 4). Hsp70s function in concert with a cochaperone, called DnaJ or Hsp40. For example, the *Escherichia coli* Hsp70 protein DnaK requires DnaJ to function in the initiation of bacteriophage λ DNA replication (5). DnaJ increases the ATPase activity and modulates substrate binding of Hsp70 (6) and is required for Hsp70 function *in vivo*. Cells contain multiple DnaJ family members, and, in some cases, a specific DnaJ is required for a particular Hsp70 to function (7). Despite the key role of DnaJ in Hsp70 function, little is known about the Hsp70 determinants that mediate binding to DnaJ. A very recent NMR study localizes one binding determinant to the ATPase domain of DnaK (8).

E. coli DnaJ is comprised of a J-domain, a glycine–phenylalanine rich segment, a cysteine rich segment, and a C-terminal region, of which the J-domain is the most important (9). The J-domain defines this family of proteins, and some members contain only this domain. The NMR structure of this domain has been determined (10, 11). A primary binding determinant to Hsp70 is widely believed to be a universally conserved tripeptide, His–Pro–Asp, located in the loop between helices II and III of the J-domain (12, 13). Point mutations in this tripeptide abolish binding of DnaJ to DnaK (14); mutations in this tripeptide also abolish function of the eukaryotic J-domains in Sec63 and simian virus 40 T antigen (15, 16). To map the sites in DnaK that bind to the J-domain, we searched for allele-specific suppressors of *dnaJ* mutations located in the invariant tripeptide. We have identified several *dnaK* suppressor mutants of *dnaJD35N* and studied their interactions with DnaJ *in vitro*, using the BIAcore based on surface plasmon resonance (SPR) detection system (Piscataway, NJ) that allows for the direct visualization of protein–protein interactions in real time. Our results provide evidence that the lower cleft of the N-terminal ATPase domain is a binding pocket for the J-domain. A recent study shows (17) that the J-domain alone does not stimulate the ATPase activity of DnaK but that stimulation is restored by the addition of a DnaK substrate peptide along with the J-domain. These results raised the possibility that DnaJ itself might interact with the DnaK peptide-binding site. To pursue this further, we have examined the ability of DnaK C-terminal mutations (18) in the vicinity of the substrate-binding site to bind to DnaJ. Our results suggest that DnaJ exhibits bipartite binding to the Hsp70 molecular chaperone DnaK.

MATERIALS AND METHODS

PCR-Based Mutagenesis and Selection of DnaK Suppressor Mutants. Random mutagenesis of the entire *dnaK* gene was performed by PCR with *Taq* DNA polymerase by using a 5′-primer introduced *Afl*III site that is compatible with *Nco*I site for ligation and a 3′-primer introduced *Bam*HI site. The PCR reactions contained 10 mM Tris·HCl (pH 8.3), 50 mM KCl, 10 ng of pNRK416, 50 pmol of each primer, 0.2 mM dNTPs, 1.5 mM $MgCl_2$, and 2.5 units of *Taq* polymerase. pNRK416 carrying wild-type (wt) *dnaK* obtained from T. Yura (Kyoto Research Park, Japan) was used as a template for PCR. The randomly mutagenized *Afl*III–*Bam*HI *dnaK* PCR fragments were inserted into *Nco*I–*Bam*HI sites of the isopropyl-

Abbreviations: SPR, surface plasmon resonance; IPTG, isopropyl-β-D-thiogalactopyranoside; wt, wild type; bccp, biotin carboxyl carrier protein.

‡Present address: Department of Biology, Massachusetts Institute of Technology, Cambridge, MA 02139.
§To whom reprint requests should be addressed at present: Departments of Microbiology and Stomatology, 513 Parnassus, Box 0512, University of California, San Francisco, CA 94143. e-mail: cgross@cgl.ucsf.edu.

The publication costs of this article were defrayed in part by page charge payment. This article must therefore be hereby marked "*advertisement*" in accordance with 18 U.S.C. §1734 solely to indicate this fact.

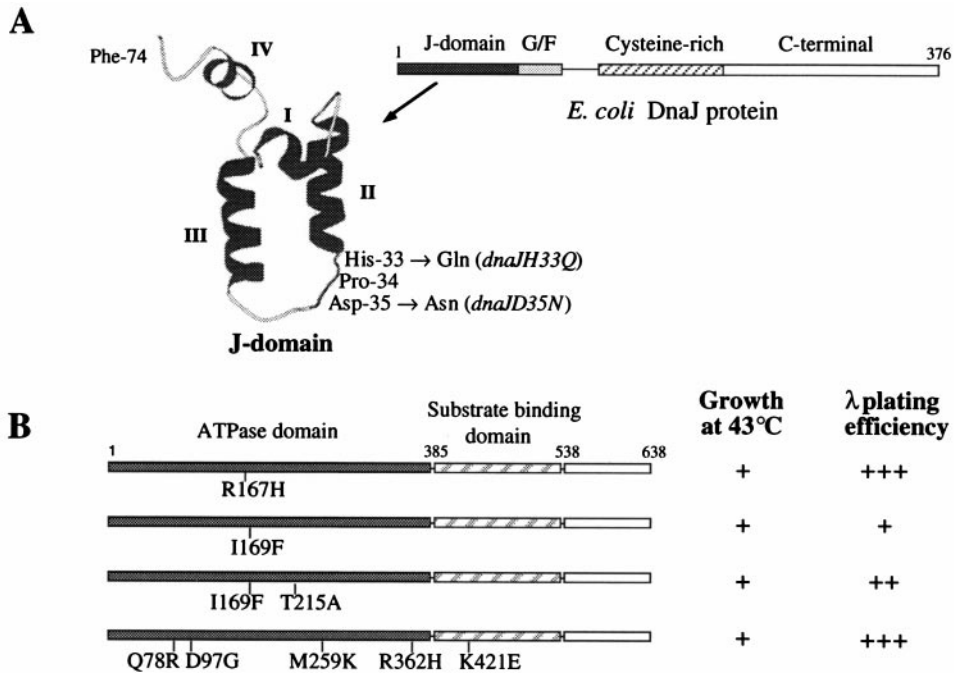

FIG. 1. (*A*) The location of *dnaJD35N* and *dnaJH33Q* mutations. A schematic of *E. coli* DnaJ with a representation of the NMR structure of the J-domain indicating the location of His-33 → Gln and Asp-35 → Asn, the two point mutations in the universally conserved tripeptide that abolish binding to DnaK. (*B*) Characterization of growth phenotypes of the allele-specific *dnaK* suppressors of *dnaJD35N*. *dnaJD35N* was transformed with a plasmid containing each suppressor and tested for growth at 43°C and λ-plating efficiency at 30°C. +, growth at 43°C; −, no growth at 43°C, and +++, ≈300 λ plaque-forming units and ≈220 λ progeny per infected cell; ++, ≈230 pfu and ≈75 λ progeny per infected cell; +, ≈200 very small plaques and ≈30 λ progeny per infected cell; −, no λ growth. For comparison, *dnaJD35N* exhibited no growth at 43°C or λ plating when the plasmid encoded wt *dnaK*. The isogenic wt strain (MC1061) exhibited growth at 43°C and +++ λ-plating efficiency.

β-D-thiogalactopyranoside (IPTG)-inducible *ptrc* vector (Invitrogen) containing the *lacI*^{q} gene and transformed into *dnaJD35N* (CAG25025) or *dnaJH33Q* (CAG13094) by electroporation. Transformants were selected on Luria–Bertani-ampicillin plates at 43°C and then screened for those able to propagate bacteriophage λ. Suppressors were selected in the absence of inducer because expression of wt *dnaK* under the control of *ptrc* promoter in the absence of IPTG was sufficient to complement the *dnaK756* mutation. Suppressor-containing plasmids were purified and retransformed into *dnaJD35N*, *dnaJH33Q*, and Δ*dnaJ* (CAG13718) strains to assess allele-specific suppression. The λ plating efficiency and the progeny burst size of the *dnaJ* mutant strain containing the *dnaK* suppressor were determined as described previously (19).

Plasmids. For the BIAcore-binding experiment, a translational fusion of the carboxyl-terminal 85 amino acids of the biotin carboxyl carrier protein (bccp) to the C terminus of DnaJ was constructed in pET15B (Novagene). Expression of this fusion gene is under the control of an IPTG-inducible promoter. This carboxyl-terminal domain of bccp is sufficient to allow biotinylation of the fusion protein (20). The PCR-generated *dnaJ* fragment with 3′- and 5′-primers that introduced the *Nco*I and *Bam*HI sites, respectively, was cloned into the *Nco*I–*Bam*HI sites of the pET15B, and then the PCR-generated bccp gene encoding the carboxyl-terminal 85 amino acids was inserted into the *Bam*HI site of the recombinant plasmid above to generate pWCS14. The mutant *dnaJD35N–bccp* fusion (pWCS26) was constructed by swapping the PCR-generated *Nco*I–*Dra*III mutant fragment with the wt fragment of pWCS14. Plasmid pWCS33 encoding wt *dnaK* under control of the IPTG-inducible *ptrc* promoter was constructed by inserting the *Afl*III–*Bam*HI *dnaK* PCR fragments into *Nco*I–*Bam*HI sites of the pQE60 vector (Qiagen, Chatsworth, CA), followed by cloning the *dnaK* His-tagged gene of the recombinant plasmid into the expression plasmid pTrcHisA (Invitrogen) containing the *lacI*^{q} gene. The sequences of the PCR-amplified fragments were confirmed by the dideoxynucleotide sequencing.

Site-Directed Mutagenesis. Point mutations in the DnaK ATPase domain (N147A, D148A, Q152A, R167A, I169A, N170A, T173A, and Q378A) were obtained by oligonucleotide-directed mutagenesis by using the "megaprimer" method (21). The PCR segment carrying each mutation was swapped with the corresponding segment in the His-tagged wt *dnaK* (pWCS33) and then verified by DNA sequencing.

Production and Purification of Proteins. Proteins were produced in *E. coli* strain BL21(DE3). Cells were grown at 37°C to mid-log at which time expression of proteins were induced with 1 mM IPTG for 3 hr. Cell lysates were prepared essentially as described previously (22) and the His-tagged proteins were purified as described in the Qiagen protocol. Peak fractions containing DnaK were pooled and dialyzed against buffer of 50 mM Hepes/KOH (pH 7.6), 50 mM KCl, 10 mM $MgCl_2$, and 1 mM DTT. If necessary, proteins were further purified by chromatography through an ATP-agarose column (Sigma) as described previously (22).

SPR Detection of DnaK–DnaJ Interaction. The BIAcore biosensor system (Biacore) (23) was used to measure the relative affinity and kinetics of the interaction between DnaK and DnaJ. Kinetic values obtained are relative because of geometric considerations. We immobilized DnaJ to a streptavidin-coupled sensor chip via a biotin group on the biotin carboxyl carrier protein (bccp) fused to the C-terminus of DnaJ. The DnaJ–bccp fusion protein was functionally active because the fusion protein complemented the growth defect of a Δ*dnaJ* strain. Streptavidin was immobilized through the primary amines to the sensor surface according to the procedure described (23). All binding experiments were performed at 25°C in 50 mM Hepes/KOH (pH 7.6), 50 mM KCl, 10 mM $MgCl_2$, and 0.003% surfactant P-20 with a flow rate of 4 μl min^{-1}. Because the interaction of DnaK and DnaJ is ATP-dependent, DnaK (1 μM) was preincubated in 50 mM Hepes/

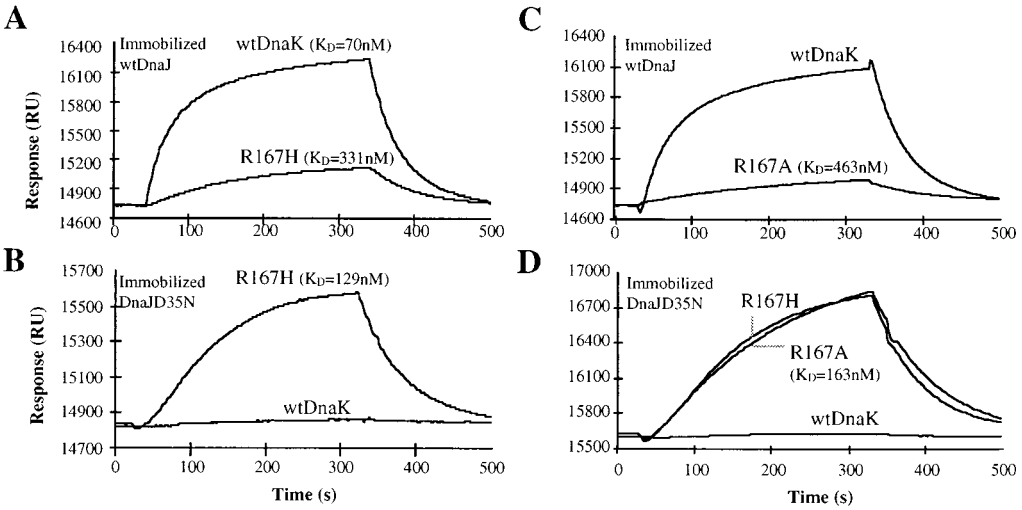

E *In vivo* phenotypes in *dnaJD35N* strain

Plasmid	Growth at 43 °C	λ plating efficiency
wtDnaK	–	–
R167H	+	+++
R167A	–	++

FIG. 2. Surface plasmon resonance detection of the interaction of wt DnaK, DnaK R167H, and DnaK R167A with wt DnaJ or DnaJD35N. An increase in resonance units (RU) indicates binding in real time of the injected DnaK protein to DnaJ protein immobilized on the sensor chip. The dissociation equilibrium constants ($K_D = k_d/k_a$) are the means of three to seven independent experiments. (*A*) Interaction of wt and R167H DnaK with immobilized wt DnaJ. (*B*) Interaction of wt and R167H DnaK with immobilized DnaJD35N. (*C*) Interaction of wt and R167A DnaK with immobilized wt DnaJ. (*D*) Interaction of R167H and R167A DnaK with immobilized DnaJD35N. (*E*) *In vivo* phenotypes of a *dnaJD35N* strain bearing plasmids encoding wt DnaK, R167H DnaK, or R167A DnaK performed as described in Fig. 1*B*.

KOH (pH 7.6), 50 mM KCl, 10 mM $MgCl_2$, 1 mM EDTA, and 1 mM ATP at 25°C for 5 min and then injected over DnaJ (1,000–1,500 resonance units, corresponding to ≈1.0–1.5 ng mm^{-2}). The residual plots for fitting the DnaK–DnaJ-binding curves indicated that the curves fit better to a double exponential than to a single exponential. However, the rate constants determined by fitting to a double exponential were irreproducible, suggesting that the biphasic effect might be caused by possible rebinding of DnaK. Hence, we used a monophasic model utilizing only the initial portion of the dissociation phase to avoid the possible rebinding of DnaK. The fit to this monophasic model was acceptable. Equilibrium association and dissociation constants were deduced from the rate constants.

RESULTS

Selection of *dnaK* Suppressor Mutants. We have embarked on a search for *dnaK* mutants that are allele-specific suppressors of two different *dnaJ* mutations, *dnaJH33Q* and *dnaJD35N*. These mutations are in the universally conserved tripeptide located in the surface loop of J-domain (Fig. 1*A*). As these *dnaJ* mutants are unable to grow above 42°C or propagate bacteriophage λ at any temperature, we looked for mutations in PCR-mutagenized *dnaK* that restored growth at 43°C and then screened among these for mutants allowing λ growth. We have identified three *dnaK* mutants (frequency of 10^{-6}) that suppressed *dnaJD35N*, but not *dnaJH33Q* or Δ*dnaJ*, indicating that they were allele specific suppressors. No suppressors of *dnaJH33Q* were identified. As each *dnaK* suppressor contained multiple mutations, we located amino acid residue(s) involved in the suppression by fragment swaps between the suppressors and wt *dnaK*, followed by DNA sequencing of the entire mutagenized region present in otherwise wt *dnaK*. Two *dnaK* suppressor alleles with the single amino acid changes R167H and I169F exhibited full and partial suppression respectively. A third allele required the combined effects of multiple mutations (Q78R, D79G, M259K, R362H, and K421E) for suppression (Fig. 1*B*). Suppression by I169F was enhanced by a second mutation, T215A. Interestingly, both R167H and I169F are highly conserved and located in the lower cleft of the DnaK ATPase domain, and T215A is located in the lower cleft as well. These genetic data strongly suggest that the N-terminal ATPase domain of DnaK contains a binding site for DnaJ.

Interaction of DnaJ with the DnaK ATPase Domain. If allele-specific suppression results from amino acid changes in DnaK that restore contacts with DnaJD35N, then they might bind better to DnaJD35N than to wt DnaJ. To test this prediction, we measured relative binding constants by using the BIAcore (Fig. 2), which is based on SPR detection. Of the three mutants tested, only R167H meets this criterion, binding ≈3-fold tighter to DnaJD35N than to wt DnaJ (compare Fig. 2*A* with Fig. 2*B*). To investigate further the role of R167 in the interaction of DnaK with DnaJ, we truncated the side chain of R167 by alanine substitution mutagenesis. The single mutation from Arg to Ala at position 167 of DnaK results in a 6-fold loss in DnaJ binding, confirming the importance of this residue in the interaction between the two proteins (Fig. 2*C*). We then used R167A to ask whether H167 recognizes N35 of DnaJD35N directly. There is no significant difference in the dissociation equilibrium-binding constants of R167H and R167A to DnaJD35N (Fig. 2*D*), indicating that a direct binding interaction is unlikely. However, their *in vivo* phenotypes indicate that the two substitutions are not equivalent (Fig. 2*E*). Whereas R167H fully suppresses the defects of DnaJD35N, R167A only partially supports λ plating and does not restore growth at 43°C. Hence, although the histidine residue does not

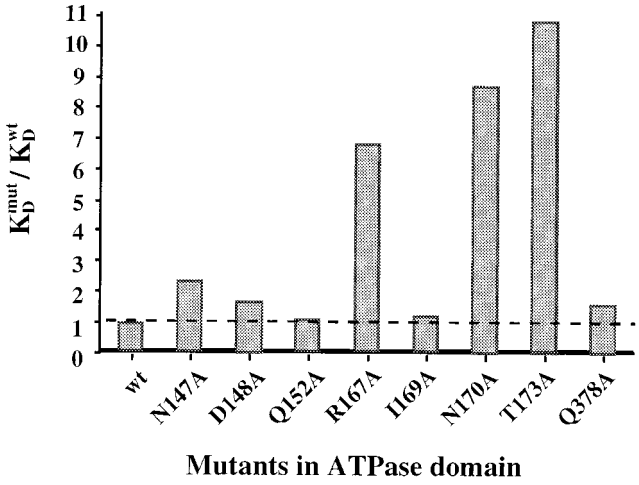

FIG. 3. Effect of the mutations in DnaK ATPase domain on the binding to DnaJ. Data are shown as the ratio of the dissociation equilibrium constants ($K_D = k_d/k_a$) of the mutants as compared with that of the wt (K_D = 70 nM). Data were determined by SPR and represent the average of at least three independent experiments.

contribute net binding energy to the interaction with DnaJD35N, it is necessary for a fully functional interaction.

To define further the individual amino acid side chains in this region of DnaK that are important for interaction with DnaJ, we truncated the surface exposed residues around R167 using alanine-scanning mutagenesis. Alanine substitution of two residues, N170 or T173, decreased binding to DnaJ ≈10-fold (Fig. 3). N170, T173, and R167 are clustered within the lower cleft of the ATPase domain, suggesting that this cleft region is a binding pocket for the J-domain flexible loop containing the invariant tripeptide. An electrostatic surface potential diagram (Fig. 4) is consistent with this idea. It identifies the groove between the two subdomains of the ATPase domain, in which N170 and T173 are located, as the most likely candidate for a DnaJ-binding pocket because it has a cluster of negatively charged residues adjacent to R167 that could interact with positively charged residues located in the J-domain helix II. R167 that is highly conserved among various organisms could interact electrostatically with D35 of DnaJ. A recent NMR experiment examining binding of ^{15}N-labeled DnaJ2–75 to DnaK is consistent with the idea that the invariant peptide in the flexible loop, especially D35, as well as residues located in the outer surface of helix II, interact with DnaK ATPase domain (8). A completely independent approach, reported in the accompanying manuscript also argues that the lower cleft of the ATPase domain of DnaK binds to DnaJ (27).

Interaction of DnaJ with the DnaK Substrate-Binding Domain. Although the J-domain alone cannot stimulate the ATPase activity of DnaK, addition of a DnaK substrate restores stimulation (17), raising the possibility that DnaJ itself might interact with the DnaK substrate-binding site. We therefore tested a set of seven DnaK mutations (18) in the vicinity of the peptide-binding site for DnaJ binding (Fig. 5). Of these, two (G400D and G539D) had previously been found to have an increased K_D for binding the peptide NR (NR-LLLTG), one (D526N) exhibits altered kinetics of interaction with peptide NR without affecting the K_D (W.F.B. and M.E.G., unpublished data) and the remaining four mutants have little or no effect on peptide NR binding. The interactions of these mutant DnaKs with DnaJ mirrors their interactions with peptide. Only the two DnaK mutants (G400D and G539D) with an altered K_D for binding peptide exhibited an altered K_D for binding to DnaJ. Moreover, G400D, which had the more

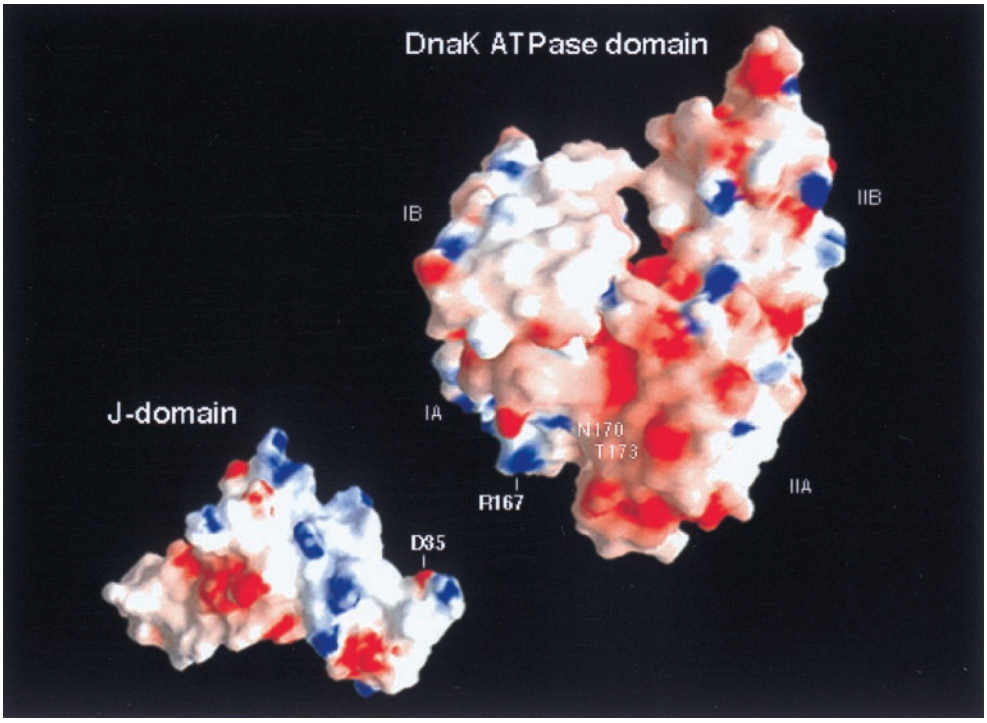

FIG. 4. Electrostatic surface potentials of the ATPase domain of DnaK (PDB ID code 1DKG) (24) with A167 modeled to R167 by using the program O (25) and the J-domain of DnaJ (PDB ID code 1XBL) (11). Areas of positive and negative charges are colored blue and red, respectively. The electrostatic surface potentials were calculated and displayed by using the program GRASP (26). Residue 167 in the original PDB file is Ala instead of Arg (commonly used if the density for a residue is hard to define). The difficulty in identifying the density of residue 167 indicates that this residue is disordered. The high mobility of this residue suggests that residue 167 is not involved in intramolecular interaction within the DnaK ATPase domain but could be involved in intermolecular interaction with the D35 located in the J-domain. The groove between the IA and IIA subdomains of the ATPase domain has a patch of negative electrostatic surface potential, which is likely a potential binding pocket for the exposed positively charged residues on helix II of the DnaJ J-domain.

severe peptide binding defect, also had a slightly more severe defect in DnaJ binding. Most significantly, D526N, which exhibited an ≈20-fold increase in the on/off rates for substrate peptide without affecting the K_D of the reaction (W.F.B. and M.E.G., unpublished data), also shows an ≈3-fold increase in the on/off rates for DnaJ without affecting the K_D of this interaction (Table 1). The most likely interpretation of these data is that DnaJ makes contact in the C-terminal substrate-binding domain of DnaK. We believe that the alternative interpretation, attributing the DnaJ-binding defects to altered interaction of DnaJ with the ATPase domain, is considerably less likely. The substrate-binding defects of these DnaK mutants observed in the isolated C-terminal fragments, arguing that the defects do not arise from altered interdomain interaction. Moreover, it is difficult to adequately explain the phenotype of D526N, the enhanced rate mutant with this interpretation. None of these mutations in the substrate-binding domain of DnaK alter specific DnaK-peptide contacts, so we cannot distinguish whether DnaJ binds to the substrate-binding site itself or in close proximity to this site. Some substrates, such as λP protein (28), are believed to bind first to DnaJ and then be transferred to DnaK. Binding of DnaJ in the vicinity of the substrate-binding site could facilitate transfer of substrate polypeptide from DnaJ to DnaK.

DISCUSSION

Our genetic and biochemical data suggest that DnaJ interacts with at least two distinct sites on DnaK. The invariant tripeptide in the flexible loop of the J-domain binds to the underside of the ATPase domain in a cleft between the two subdomains; and another part of the J-domain or another region of DnaJ binds at or near the DnaK substrate-binding site. Binding of DnaJ to DnaK is dependent on both ATP binding (29) and the consequent conformational changes of DnaK (W.-C.S. and C.A.G., unpublished data). ATP binding to the ATPase domain of Hsp70 or DnaK induces subtle conformational changes in the N-terminal ATPase domain followed by significant conformational changes in the C-terminal substrate-binding domain through the interdomain communication. We argue that the ATP-induced conformational changes in both domains are required for binding of DnaJ to DnaK.

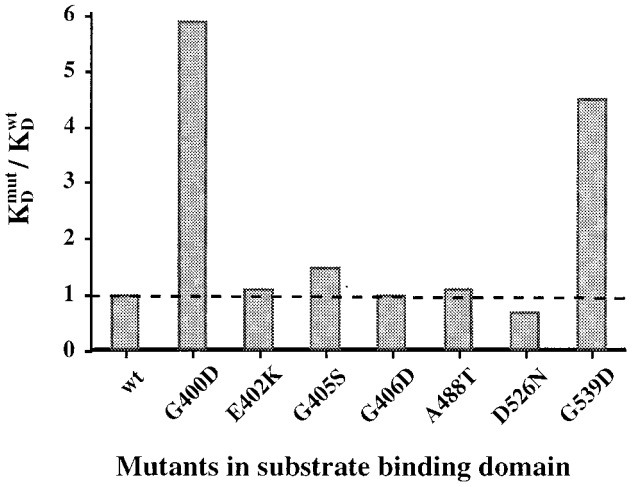

FIG. 5. Effect of the mutations in DnaK substrate-binding domain on the binding to DnaJ. Data are shown as the ratio of the dissociation equilibrium constants ($K_D = k_d/k_a$) of the mutants as compared with that of the wt (K_D =70 nM). Data were determined by SPR and represent the average of at least three independent experiments. These mutants were originally selected because they alleviated the toxicity of an overexpressed C-terminal fragment of DnaK (18). Their dissociation equilibrium-binding constants for peptide NR indicated that two mutants, G400D (K_D >150 μM) and G539D (K_D = 30 μM) had K_Ds that were significantly increased relative to the wt value of 11 μM. The remainder of the mutants exhibited binding constants that were different from that of the wt by 50% or less.

Table 1. Comparison of apparent association and dissociation rate constants (k_a, k_d) between wt and D526N DnaK for the interaction with immobilized wt DnaJ

	Apparent k_a, M^{-1} s^{-1}	Apparent k_d, s^{-1}	Apparent K_D, nM
wtDnaK-DnaJ	2.3 (±0.2) × 10^4	1.6 (±0.1) × 10^{-3}	70 (±10)
D526N-DnaJ	8.2 (±4.6) × 10^4	4.0 (±1.1) × 10^{-3}	50 (±19)

Data were determined by SPR and are the average of at least three independent experiments.

The ATPase domain of Hsp70 is homologous in its three dimensional structure to those of actin and hexokinase, both of which undergo subdomain rearrangement after binding ATP (30). If the ATPase subdomains of DnaK are similarly reoriented upon ATP binding, the DnaJ-binding cleft between the subdomains of the ATPase domain could be exposed. Arguing for such a rearrangement is the fact that domain IIB in bovine Hsc70-ADP is rotated 14° compared with its position in a nucleotide free DnaK–GrpE complex. Although this conformational change has been attributed to complexation with GrpE (24), it also could be caused by subdomain rearrangement between the nucleotide free and bound states of DnaK.

Our data suggest that DnaJ binding to the substrate-binding domain also may require an ATP-induced conformational change. Upon binding ATP, the substrate-binding domain of DnaK shifts from a "closed" to an "open" form permitting rapid substrate binding (4, 31, 32). Increased accessibility to substrate has been suggested to result from opening an α-helical "lid" covering the β-sandwich substrate-binding region. The D526N mutant is proposed to increase the on-rate for substrate by affecting lid opening, thus mimicking the effect of ATP (W.F.B. and M.E.G., unpublished data). Because this mutant increases the on-rate for DnaJ, it is very likely that ATP binding also exposes the C-terminal DnaJ-binding site.

We suggest that DnaJ binding leads to further conformational changes in both domains of Hsp70. Binding of the invariant peptide located in the disordered loop to the inter-subdomain cleft is likely to require an induced fit mechanism (11) and could propagate a conformational change either directly or indirectly (through the coupling with the substrate-binding domain) to the nearby ATP catalytic center that would facilitate ATP hydrolysis. Binding of DnaJ in the vicinity of the substrate-binding pocket may enhance substrate transfer to Hsp70 as well as alter substrate binding/release properties either by direct interaction or by an allosteric mechanism. Most importantly, the dual binding of DnaJ to Hsp70 may facilitate signaling between the two key domains of Hsp70. Such interactions may underlie the functional specificity of some DnaJ–Hsp70 pairs.

We thank J. Wild for providing strain *dnaJD35N*, Dr. B. Bukau for sharing unpublished results, Dr. D. A. Agard, M. Lonetto, and C. Chan for helpful discussions, W. Lau for initial BIAcore experiments, and members of the Gross laboratory, Dr. W. A. Hendrickson and Dr. E. Blackburn for critical reading of the manuscript. Supported by a National Institutes of Health Grant GM36278-13.

1. Hartl, F.-U. (1996) *Nature (London)* **381,** 571–580.
2. Morimoto, R., Tissieres, A. & Georgopoulos, C. (1994) *The Biology of Heat Shock Proteins and Molecular Chaperones* (Cold Spring Harbor Lab. Press, Plainview, NY).
3. Flaherty, K. M., DeLuca-Flaherty, C. & McKay, D. B. (1990) *Nature (London)* **346,** 623–628.
4. Zhu, X., Zhao, X., Burkholder, W. F., Gragerov, A., Ogata, C. M., Gottesman, M. E. & Hendrickson, W. A. (1996) *Science* **272,** 1606–1614.
5. Alfano, C. & McMacken, R. (1989) *J. Biol. Chem.* **264,** 10709–10718.

6. Bukau, B. & Horwich, A. L. (1998) *Cell* **92,** 351–366.
7. James, P., Pfund, C. & Craig, E. A. (1997) *Science* **275,** 387–389.
8. Greene, M. K., Maskos, K. & Landry, S. J. (1998) *Proc. Natl. Acad. Sci. USA* **95,** 6108–6113.
9. Kelley, W. L. (1998) *Trends Biochem. Sci.* **23,** 222–227.
10. Szyperski, T., Pellecchia, M., Wall, D., Georgopoulos, C. & Wüthrich, K. (1994) *Proc. Natl. Acad. Sci. USA* **91,** 11343–11347.
11. Pellecchia, M., Szyperski, T., Wall, D., Georgopoulos, C. & Wüthrich, K. (1996) *J. Mol. Biol.* **260,** 236–250.
12. Wall, D., Zylicz, M. & Georgopoulos, C. (1995) *J. Biol. Chem.* **269,** 5446–5451.
13. Tsai, J. & Douglas, M. G. (1996) *J. Biol. Chem.* **271,** 9347–9354.
14. Wall, D., Zylicz, M. & Georgopoulos, C. (1995) *J. Biol. Chem.* **270,** 2139–2144.
15. Scidmore, M. A., Okamura, H. H. & Rose, M. D. (1993) *Mol. Biol. Cell* **4,** 1145–1159.
16. Kelley, W. L. & Georgopoulos, C. (1997) *Proc. Natl. Acad. Sci. USA* **94,** 3679–3684.
17. Karzai, A. W. & McMacken, R. (1996) *J. Biol. Chem.* **271,** 11236–11246.
18. Burkholder, W. F., Zhao, X., Zhu, X., Hendrickson, W. A., Gragerov, A. & Gottesman, M. E. (1996) *Proc. Natl. Acad. Sci. USA* **93,** 10632–10637.
19. Georgopoulos, C. P. & Herskowitz, I. (1971) in *The Bacteriophage Lambda*, ed. Hershey, A. D. (Cold Spring Harbor Lab. Press, Plainview, NY), pp. 553–564.
20. Cronan, J. E., Jr. (1990) *J. Biol. Chem.* **265,** 10327–10333.
21. Sarkar, G. & Sommer, S. S. (1990) *BioTechniques* **8,** 404–407.
22. Kamath-Loeb, A. S., Lu, C. Z., Suh, W.-C., Lonetto, M. A. & Gross, C. A. (1995) *J. Biol. Chem.* **270,** 30051–30059.
23. Johnsson, B., Löfås, S. & Lindquist, G. (1991) *Anal. Biochem.* **198,** 268–277.
24. Harrison, C. J., Hayer-Hartl, M., Liberto, M. D., Hartl, F.-U. & Kuriyan, J. (1997) *Science* **276,** 431–435.
25. Jones, T. A., Zou, J. Y., Cowan, S. W. & Kjeldgaard, M. (1991) *Acta Crystallogr. A* **47,** 110–119.
26. Nicholls, A., Sharp, K. A.& Honig, B. J. (1991) *Proteins* **11,** 281–296.
27. Gässler, C. S., Buchberger, A., Valencia, A. & Bukau, B. (1998) *Proc. Natl. Acad. Sci. USA* **95,** 15229–15234.
28. Hoffmann, H. J., Lyman, S. K., Lu, C., Petit, M.-A. & Echols, H. (1992) *Proc. Natl. Acad. Sci. USA* **89,** 12108–12111.
29. Wawrzyn, A. & Zylicz, M. (1995) *J. Biol. Chem.* **270,** 19300–19306.
30. Holmes, K. C., Sander, C. & Valencia, A. (1993) *Trends Cell Biol.* **3,** 53–59.
31. Buchberger, A., Theyssen, H., Schröder, H., McCarty, J. S., Virgallita, G., Milkereit, P., Reinstein, J. & Bukau, B. (1995) *J. Biol. Chem.* **270,** 16903–16910.
32. Schmid, D., Baici, A., Gehring, H. & Christen, P. (1994) *Science* **263,** 971–973.